ISBN: 978-3-95450-233-2 ISSN: 2673-5504 doi:10.18429/JACoW-SRF2021-TUPTEV010

CAMERA PLACEMENT IN A SHORT WORKING DISTANCE OPTICAL INSPECTION SYSTEM FOR RF CAVITIES

A. Luthi*, L. Buonocore, M. Di Castro, H. Gamper[1], A. Macpherson†
CERN, Geneva, Switzerland
[1] also at Institute of Robotics, Johannes Kepler University, Linz, Austria

Abstract

Inspection of the RF surface of cavities for the purpose of detecting surface anomalies has been well established, and is typically based on long working distance optical systems using on-axis camera and mirror systems to scan the cavity surface. In order to improve the systematic inspection of the full RF surface of large area cavities, a novel short working distance inspection system is being developed at CERN. This new system is based on a mechatronic robotic system to position that camera at normal incidence close to the cavity surface. To accommodate working distance fluctuations, and to provide increased depth of field resolution, the short working distance camera is coupled with a liquid lens focusing system, providing a programmable focusing function. Details of inspection bench design and first results are reported, as well as details on camera positioning optimisation and the proximity detection surveillance for collision-free scanning of the full-cavity surface.

INTRODUCTION

Inspection of the surface of RF cavities has been a well-established activity throughout SRF community with different laboratories adopting various technical solutions that matched individual needs and cavity geometries. These systems have had considerable success with spot inspection and classification of defects, as well as weld assessment and other such localised surface inspection. Typically, due to the difficulty in accessing the RF surface of a cavity, imaging solutions have opted for long focal length imaging systems. Cavity inspection systems on long working distance imaging with the camera positioned on the beam axis and the camera-to-surface optical path defined by a mirror system being well established, with the KEK-Kyoto system [1] an excellent example of this approach. More recent developments by KEK [2], and the DESY OBACHT - Optical Bench for Automated Cavity inspection with High resolution on short Timescales - system [3] show the ongoing development within the community, and the Jefferson Laboratory (JLab) very long distance microscope a mirror system, with the camera external to the cavity [4] is a balance of mechanical simplicity relative to optical complexity.

However, while such long working distance microscopes provide a simpler mechanical solution, there are issues with limited field of view at high resolution, full scanning coverage of the RF surface, image distortion due to non-normal incidence of the camera on the imaging surface, and lighting artifacts due to remote lighting sources. In order to address these concerns, an alternative approach is adopted, with a short working distance optical inspection system under development at CERN. This system uses a mechatronic robotic positioning of a camera at normal incidence, and at short working distance from the cavity surface. This system is designed for reproducible positional scanning of all the present set of axially symmetric cavities in the CERN inventory, ranging from large aperture 400 MHz LHC cavities, to 704 MHz 5-cells and small aperture 1.3GHz single cell elliptical cavities. Here, CERN has opted for a camera placement system that is producing images of uniform depth of field and image-wide field of view, in order to build a fully imaged mosaic of the entire cavity surface. To this end the top-level user requirements for this new inspection system [5] can be summarised as:

1. The entire cavity inner surface has to be scanned.
2. The system must be able to achieve reproducible camera positioning for imaging.
3. An image overlap between consecutive photos has to be ensured, with a target overlap of 30%.
4. The full scan for each cavity type has to be performed in less than 12 hours.
5. Imaging resolution of 10 µm is required.

In order to achieve this, a novel robotic arm based imaging system has been developed, and in what follows below, we detail the design and development of this mechatronic system.

CAMERA POSITIONING BY ROBOTIC ARM

In order to scan the RF surface with a short working distance camera, the camera positioning has to be carefully arranged for each imaging position, such that imaging requirements are met (i.e. achievable focus at normal incidence) and with no risk of the camera positioning system contacting the inner surface of the cavity at any point. To ensure this for a robotic arm system on an axially symmetric cavity, a 2D path of the camera arm has to be computed and evaluated in advance; for the dimension in the azimuth, axial symmetry along the beam axis implies that only a 2D path evaluation is necessary, as scanning is performed by cavity rotation around the beam axis.

* adrien.luthi@cern.ch
† alick.macpherson@cern.ch

ISBN: 978-3-95450-233-2 ISSN: 2673-5504 doi:10.18429/JACoW-SRF2021-TUPTEV010

Camera Positioning and Path Planning

Naturally, the cavity arm path planning is based on the inner surface shape of each cavity, and the camera is positioned in such a way that the distance between the inner surface and camera is kept constant. This avoids depth of field excursions which would compromise scanning performance and/or scan coverage. To define the camera path planning, the cavities inner surfaces are reconstructed using geometric dimensions, which are sets of ellipses (e_j) and lines (l_k) (Fig. 1) [5]. Moreover, as an image overlap is required when the path is generated (nominally 30%), this defines the distance between two consecutive points (c_i and c_{i+1}) of imaging location of the reconstructed surface. At the end of this path generation process, the result is a set of equidistant points constituting the 2D image position points needed to faithfully image the surface i.e. the set of (z, r) locations in a cylindrical coordinate system, where the cavity rotation is in the azimuth (θ) direction.

Path Generation

Based on the computed scanning path, the camera position (p_i) perpendicular to its counterpart image point (c_i) can be determined from Eq. 1, where d is the distance from the camera to the inner surface, and n the normal vector of the surface y which could be either an ellipse or a line (for details see [5] and Fig. 2). By iterating on each point (c_i), all camera positions (p_i) are computed and stored. This set of camera points is then used as input to the robotic arm drive system.

$$\boldsymbol{p_i} = \boldsymbol{c_i} + d\boldsymbol{n} \tag{1}$$

with:

$$\boldsymbol{n} = \frac{\boldsymbol{c_i'}}{\|\boldsymbol{c_i'}\|} \cdot R\left(\frac{\pi}{2}\right) = \frac{\boldsymbol{c_i'}}{\|\boldsymbol{c_i'}\|} \begin{bmatrix} 0 & -1 \\ 1 & 0 \end{bmatrix} \tag{2}$$

$$\boldsymbol{c_i'} = \left(\frac{1}{\frac{\partial y}{\partial x}}\right)\Big|_{c_i} \tag{3}$$

$$\frac{\partial y}{\partial x} = \begin{cases} -\dfrac{b_j^2(x_j - x_{Cj})}{a_j^2(y_j - y_{Cj})} & \text{if } \{c_i\} \in e_j \\ m_k & \text{if } \{c_i\} \in l_k \end{cases} \tag{4}$$

Further as a point of note, the requirement that the camera operates at normal incidence to the inner surface, gives the clear requirement of an adjustable camera head orientation, and this can be seen in Eq. 5, which defines the camera head orientation β_i with respect to the beam axis of the cavity; at the cavity equator $\frac{\partial y}{\partial x} = 0$ and $\beta_{\text{equator}} = \pi/2$.

$$\beta_i = \arctan\left(\frac{\partial y}{\partial x}\right) + \frac{\pi}{2} \tag{5}$$

CAVITY SCANNING SETUP

In order to scan the RF surface of a cavity, the inspection system implemented is split into three distinct of subsystems; a fixed structure, a cavity rotation mechanism, and a mobile trolley that positions the camera inside the cavity. The latter is a stepper motor driven stage that moves along the principal axis of the cavity and houses the robotic arm and camera unit.

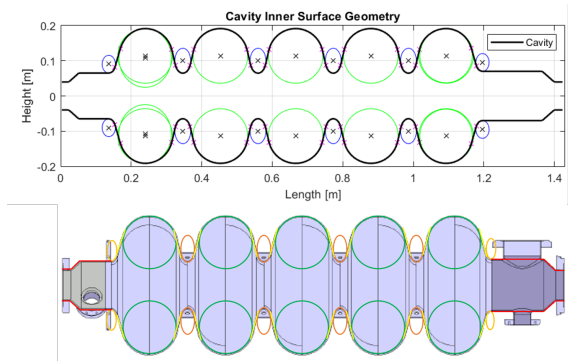

Figure 1: Example of the reconstructed profile of the 704 MHZ 5-cells cavity (top) based on the inner shape geometric structure (bottom) - ellipses (green and yellow) and lines (red and orange) sets.

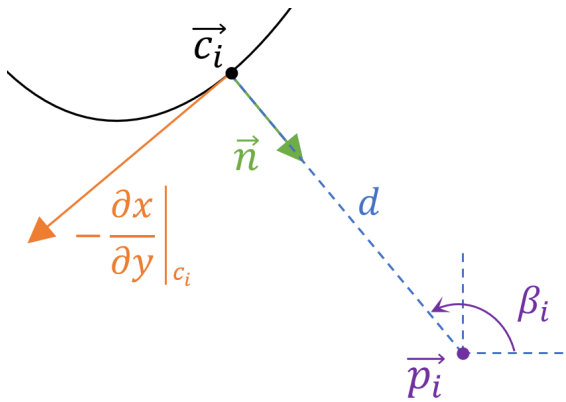

Figure 2: Path equation illustration.

To perform a full scan, an iteration of the process consists of driving the robotic arm to reach the next desired pre-computed position and to stop there. At this step, an auto focus verification is performed, followed by streamed image acquisition as the cavity is rotated through one full turn, at a speed compatible with real-time image capture and image overlap constraints. This sub-process is then repeated for each position, thereby establishing a full-cavity scan. To minimize the full process time, an angular cavity velocity is assigned to each computed position. Indeed, each angular velocity depends on the cavity's tangential velocity perceived by the camera and therefore also on the cavity's radius for each position and on the camera capabilities. Based on the geometry of CERN's 704 MHz 5-cells elliptical cavity, a full scan is foreseen taking around 9 hours and requires 18'955 image acquisitions, while for the LHC single cell 400 MHz cavity the expected time is of order 6 hours and 17'943 images.

ISBN: 978-3-95450-233-2 ISSN: 2673-5504 doi:10.18429/JACoW-SRF2021-TUPTEV010

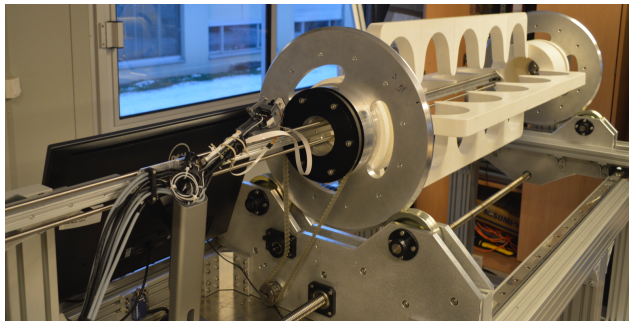

Figure 3: Prototype setup with the robotic arm and camera unit in foreground. Also visible is the 3D printed white cavity envelope used during development.

Cavity Installation System

Cavity rotation is activated through a motor mounted below the cavity with a belt transmission. End plates mounted on the cavity and flanges are used both to support the cavity and define the central reference axis for the cavity and camera system. A linear guide rail inserts along the beam axis of the cavity and is fixed to both end plates, giving a well-defined and reproducible reference axis for imaging, with a cylindrical coordinate system given by the beam axis and one of the beam port flanges. Cavity rotation is by a precision belt drive fixed to the reference end plate, which sits on simple ball-bearing based rollers (Fig. 3), and simple 1-turn consistency checks on azimuth positional accuracy is foreseen. The trolley is driven by a recirculating ball-screw (RBS) with two linear guides, with an RBS motor mounted on the rotation axis of the ball-screw. Direct control of this RBS motor allows for the camera arm to be positioned on-axis at any position over the length of the cavity. Finally, the robotic arm (Fig. 4) is a serial robot with 3 degrees of freedom, two deported motors, and one embedded. The first deported motor allows the trolley and therefore the robotic arm to move along the beam axis of the cavity. The second deported motor allows the arm to pivot in the vertical plane of the cavity while the embedded motor controls the orientation of the camera which is located at the end of the arm.

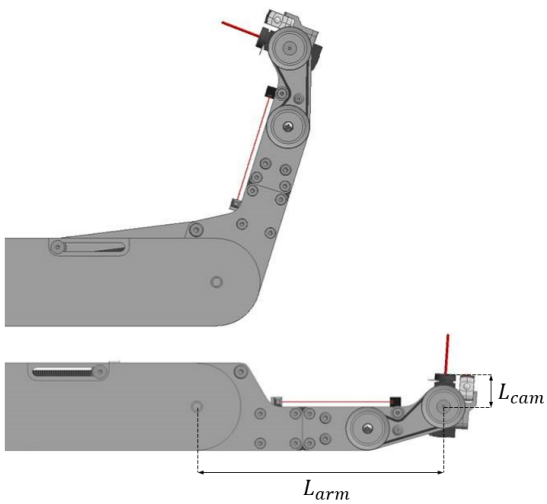

Figure 4: Robotic arm in movement with its laser beam fixed on its arm and the second laser located close to the camera.

Arm's length Optimization & Collision Avoidance

In order to image the cavity surface a full set of camera positions is predetermined based on the cavity geometry, and in theory there should be no risk of RF surface contact by the camera positioning system or any part of the robotic arm. However, as this is a short working distance system operating off-axis inside the cavity, a full anti-collision system has been integrated into the robotic arm assembly. This anti-collision system is based on two laser proximity sensors. One is used to measure the distance to the surface in front of the camera and the other is a laser beam fixed on the arm to detect proximity situations during camera positioning, with the later raising a system error if the optical circuit of the laser is interrupted. For the camera head laser, the measured distance is also used as a cross-check on the camera posi-

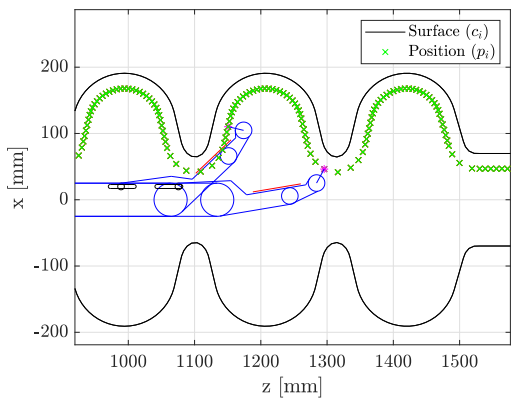

Figure 5: Robotic arm positions corresponding to maximum and minimum distance to the 5-cell 704 MHz cavity (Fig. 6)

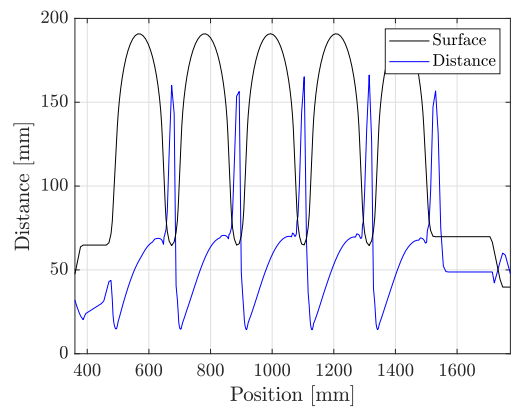

Figure 6: Closest approach distance of camera assembly shown in blue, with 5-cell cavity surface in black. The minimum closest approach for this geometry is 14 mm.

ISBN: 978-3-95450-233-2 ISSN: 2673-5504 doi:10.18429/JACoW-SRF2021-TUPTEV010

tion with respect to the surface, with compensation routines applied for any deviations within a tolerance band.

For each cavity geometry, the length of the robotic arm (L_{arm}) and of the camera (L_{cam}) (Fig. 4) are optimized for collision free inspection of cavities. To optimize these lengths, a multi-objective optimization problem [5] has been defined where the set of objective functions maximize the scanning percentage achieved for a parameter combination of L_{arm} and L_{cam}, while avoiding collision and maximizing the closest approach at each position. Simulations show the cavity specific optimization implies the need for specific robotic arms lengths - one for each cavity type. To this end, to accommodate the range of cavities under consideration at CERN, a modular robotic arm system has been developed, composed of a central arm and a cavity specific head with lasers and the camera embedded. With such optimisation, the robotic arm positions showing the maximum and minimum closest approach distance of the arm assembly are shown in Fig. 5, and the closest approach distance for a scan of the 5-cells cavity is in given in Fig. 6.

IMAGING SYSTEM

In terms of the imaging system, the camera selected is a XIMEA sub-miniature (15x15x13 mm) 18Mpix with an image size of 4896 x 3680 pixels and a pixel size of 1.25 µm. In addition, due to the tight space constraint of this project, a new technology of lens - a liquid S-mount lens from Corning - has been adopted. This liquid lens offers a compact variable focus by means of an applied voltage that modifies the lens shape, and with this camera and lens combination, the available field of view is 37 x 29°(horizontal and vertical). The prototype camera with liquid lens and laser proximity sensor is shown in Fig. 7.

Initial imaging tests with this camera on a copper 5-cell 704 MHz test cavity produced encouraging images at a working distance of 23mm as seen by the image of a weld seam and drill hole in Fig. 8. However it is evident that the strip based LED lighting array attached to the main arm axis of the robotic arm was inappropriate, as the illumination is not uniform. The lighting system is being upgraded with diffuse intensity controlled LEDs mounted on the side of the camera in order to give diffuse light with reduced reflections and shadows. As a second assessment of the camera's performance, Fig. 9 shows the image of a European 10-cent coin, with a standard camera and liquid lens settings. The insert shows a pure optical zoom with no image processing applied, and gives an idea of the achievable resolution.

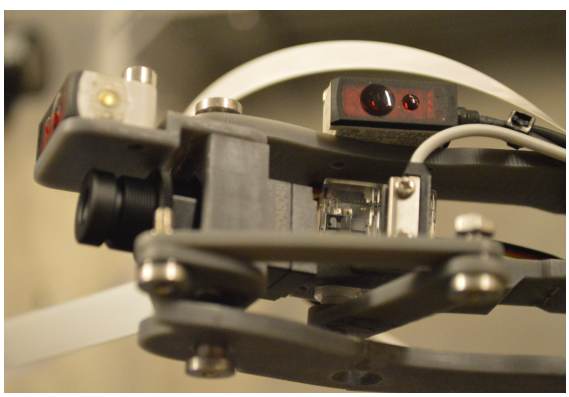

Figure 7: The sub-miniature camera assembly with liquid lens and proximity sensors.

Figure 8: Image of weld seams of a copper 704 MHZ 5-cells elliptical test cavity. The image shows details of a drilled 5mm through hole demonstrate the achievable field of view. Lighting for this image was located on the main robotic arm, and the non-uniformity across the image is apparent.

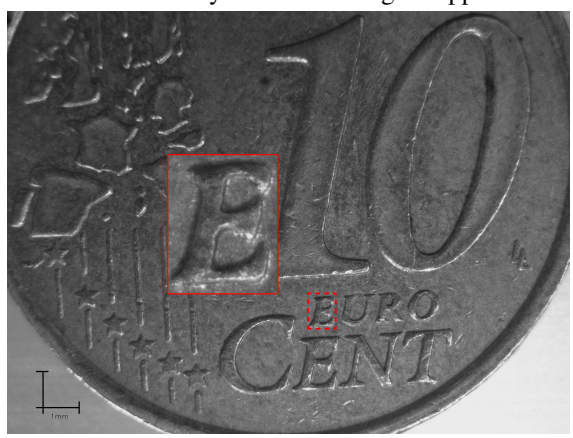

Figure 9: Photo sample of a 10 European cents coin taken at 23mm with 40V applied to the lens. Insert shows unprocessed optical zoom.

The focus functionality of the camera and lens can be quantitatively assessed in terms of a focus function based on a summed Laplacian operator evaluated over the image. This focus metric can then be evaluated as a function of liquid lens voltage, and in Fig. 10, the focusing metric as applied to Fig. 9 can be seen. Clearly, for each working distance, the liquid lens focusing range is at most 5V wide, and the available working distance (assuming for optimised lens voltage) has a peak focusing at a working distance of 22mm (Fig. 11), with a FWHM spread of 6 mm, which set the upper range of the auto-focus tolerance for the inspection system.

ISBN: 978-3-95450-233-2 ISSN: 2673-5504 doi:10.18429/JACoW-SRF2021-TUPTEV010

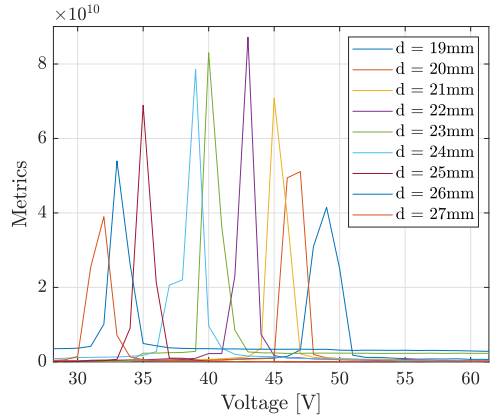

Figure 10: Metrics values over the voltage applied sorted by distance to the surface. The maximum values are clearly detectable.

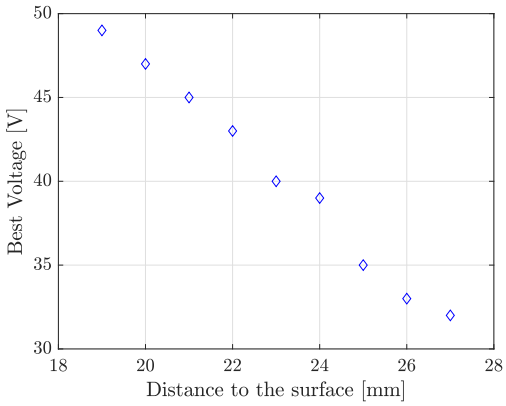

Figure 11: Best voltage values over the distance range [18-27mm] from the camera to the cavity surface.

As an additional check, the depth of field performance can be seen from the image of an ISO N10 rugosity test surface. This surface is a grooved surface with controlled surface roughness of $R_a = 12.5\mu m$. Further, this sample was a curved surface with a curvature height of 1mm. Figure 12 shows the acquired image, and it is noted that the entire image retains sufficient clarity to suggest that in addition to the $12.5\mu m$ depth of field resolution, the operation depth of field for this camera is at least 1mm of depth of field.

SUMMARY

The development of a novel cavity inspection system based on short-working distance normal incidence imaging is ongoing at CERN. User requirements for uniform and automated imaging of the full RF surface of cavities has resulted in the technological choice of a sub-miniature short working distance optical imager with an adaptive liquid lens to optimise the focusing functionality over the course of inspection scans. By employing camera positioning by robotic arm, field of view and lighting uniformity issues can be addressed, but at the cost of ensuring contact free scanning. To this end, a full laser based proximity sensor protection system has been implemented on the camera positioning structure and results demonstrate that for the cavities presently foreseen at CERN, this is no issue with the collision-free operation of the scanning system. The system is now at the stage of first scanning acquisition, and processed image scan results of a 400MHz LHC cavity are foreseen in the coming months, with machine learning-based defect detection to follow.

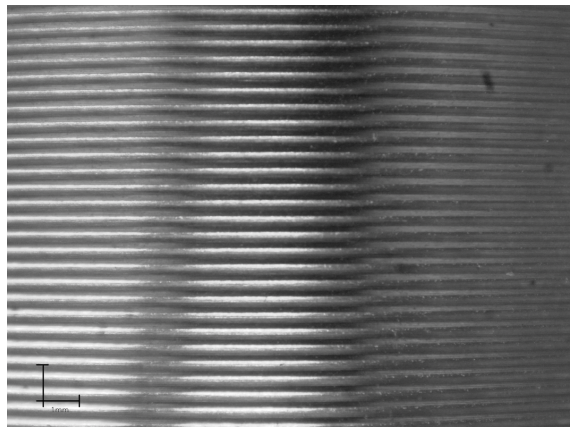

Figure 12: Photo sample of a N10 rugosity test. The height of the curvature is around 1mm. All the image is in focus meaning that the depth of field is at least 1mm.

ACKNOWLEDGEMENTS

The authors would like to thank the members of the Robotics and Mechatronics and Superconducting RF sections at CERN for their ongoing contributions to develop this system. We also would like to thank Fabrizio Pirozzi for development of the first system design, Ryan Agius for his work on the autofocus algorithm, Sergio Di Giovannantonio for his mechanical expertise on the first and second systems and Augustin Harmel for its work on the PLC control software.

REFERENCES

[1] Y. Iwashita, Y. Tajima, and H. Hayano, “Development of high resolution camera for observations of superconducting cavities”, *Phys. Rev. Spec. Top. Accel. Beams*, vol. 11, 9, pp. 1–6. Sep. 2008, doi:10.1103/PhysRevSTAB.11.093501

[2] K. Watanabe, “Review of optical inspection methods”, *Insight: Non-Destructive Testing and Condition Monitoring*, vol. 38.4, pp. 123–128, 2009.

[3] M. Wenskat, “Automated optical inspection and image analysis of superconducting radio-frequency cavities”, *J. Instrum.*, vol. 12, p. 5, 2017, doi:10.1088/1748-0221/12/05/P05016

[4] R. L. Geng and T. Goodman, “A machine for high-resolution inspection of srf cavities at Jefferson Lab", in *Proc. SRF’11*, Chicago, IL, USA, 2011, paper THPO036, pp. 798–800.

[5] A. Luthi, "Automation and optimization of a robotic system for radio frequency cavities inspection", M.S thesis, Dept. Robotic Sec., EPFL Univ., Lausanne, Switzerland, 2021.